Modeling Martian Climate with Low-Dimensional Energy Balance Models

Gareth E. Roberts

Department of Mathematics and Computer Science
College of the Holy Cross
Worcester, MA, USA

Ryan Ferraro (HC '19)
Alice Nadeau (University of Minnesota)

2019 SIAM Conference on Dynamical Systems
Snowbird, Utah
May 19–23, 2019

Figure: Spring 2018 Math and Climate seminar. Field trip to Harvard Forest.

Background on Mars

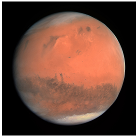 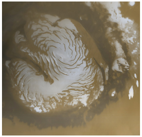 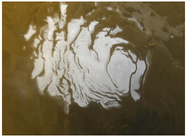 

- Thin, dry atmosphere consisting of about 95% CO_2.
- Low atmospheric pressure of 600 pascals (0.087 psi). Liquid water is unstable over most of the planet (either freezes or sublimes to vapor).
- Mean annual temperature is -63° C. Daily temperature range at the Viking 1 lander site (latitude 22.3°N) is -89° to -31°C.
- Polar ice caps exist containing a mixture of water ice and CO_2 ice. The volume of water ice in the northern ice cap is about 30% of that found in the Greenland ice sheet.
- Current Martian ice line is approximately at a latitude of 60°.

Martian Obliquity

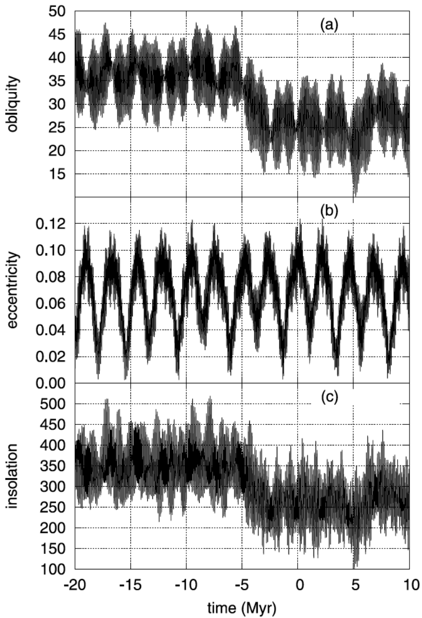

- Figure from Laskar et al., 2004. Extensive calculations show obliquity to be chaotic.
- Current obliquity of Mars is 25.19° (Earth = 23.44°)
- Average value (computed over 5 billion years) is 37.62°
- Maximum value = 82.035°; probability for obliquity > 80° is 0.015%
- Change in obliquity due to influence of secular terms in solar system

Budyko's Energy Balance Model (1969)

Basic idea: Temperature is driven by differences between energy coming in (solar radiation) and going out (outgoing longwave radiation)

Variables: $y = \sin\theta$, where θ is the usual latitude, $y \in [0, 1]$
$T = T(t, y)$, the mean annual temperature at "latitude" y.

$$R\,\frac{\partial T}{\partial t} \;=\; Q\,s(y)(1-\alpha) - (A + BT) - C(T - \overline{T})$$

$$\begin{aligned}
Q &= \text{solar constant} \\
s(y) &= \text{insolation (incoming solar radiation)} \\
\alpha &= \text{albedo (reflectivity of planet)} \\
A + BT &= \text{outgoing longwave radiation} \\
C(T - \overline{T}) &= \text{meridional heat transport} \\
\overline{T} &= \int_0^1 T(t, y)\,dy \;=\; \text{mean global annual temp.}
\end{aligned}$$

Comparison of Parameter Values

$$R\frac{\partial T}{\partial t} = Q\,s(y)(1-\alpha) - (A+BT) - C(T-\bar{T})$$

Symbol	Definition	Earth	Mars
Q	solar constant	342 W/m^2	146 W/m^2
α_r	albedo for land i.e., Martian regolith	0.32	0.25
α_s	albedo for snow/ice	0.62	0.67
$A+BT$	outgoing longwave radiation	$A = 202$ W/m^2 $B = 1.9$ W/(m^{2}C)	A unknown $B = 1.33$
$C(T-\bar{T})$	heat transport	C = 3.04	unknown

Nadeau-McGehee Insolation Approximation

Annual average insolation as a function of latitude $y = \sin\theta$ and obliquity angle β ($\gamma =$ longitude):

$$s(y,\beta) = \frac{2}{\pi^2}\int_0^{2\pi}\sqrt{1-(\sqrt{1-y^2}\sin\beta\sin\gamma-\gamma\cos\beta)^2}\;d\gamma$$

6th-degree polynomial approximation (Nadeau, McGehee 2017):

$$s(y,\beta) \approx 1 - \frac{5}{8}p_2(\tilde\beta)p_2(y) - \frac{9}{64}p_4(\tilde\beta)p_4(y) - \frac{65}{1024}p_6(\tilde\beta)p_6(y)$$

where $\tilde\beta = \cos\beta$ and p_i is the i-th Legendre polynomial

$$\begin{aligned} p_2(y) &= \frac{1}{2}(3y^2-1) \\ p_4(y) &= \frac{1}{8}(35y^4-30y^2+3) \\ p_6(y) &= \frac{1}{16}(231y^6-315y^4+105y^2-5)\,. \end{aligned}$$

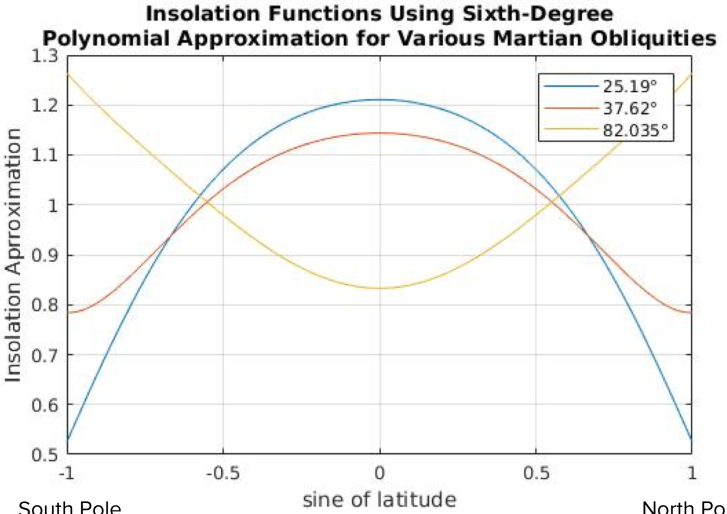

South Pole

equator

North Pole

Note: For $\beta \approx 53.937^\circ$, $s(0) = s(1)$ and $0.974 \leq s(y) \leq 1.031$ (nearly constant at 1).

Albedo and the Ice Line

Albedo varies with latitude, depending on whether the surface is ice covered in CO_2 "snow" or land.

Define the parameter $\eta \in [0, 1]$ to be the ice line, the latitudinal boundary between snow-covered ice and land.

Two-step albedo function depending on the magnitude of obliquity:

$$\alpha_1(y, \eta) = \begin{cases} \alpha_r & \text{if } y < \eta \\ \alpha_s & \text{if } y > \eta, \end{cases} \quad \text{or} \quad \alpha_2(y, \eta) = \begin{cases} \alpha_s & \text{if } y < \eta \\ \alpha_r & \text{if } y > \eta. \end{cases}$$

Left model (smaller obliquity) for polar ice caps.
Right model (large obliquity) for equatorial ice belts.
$\alpha_r \approx 0.25$ (land) and $\alpha_s \approx 0.67$ (snow-covered ice).

We will assume that $T_c = -125.5°C$ is the critical temperature at which CO_2 ice can form on Mars.

Equilibrium solutions

Let $T^* = T^*(y, \eta, \beta)$ represent the equilibrium solution of the Budyko model. Integrating the right-hand side of the PDE with respect to y from 0 to 1 yields the global mean temperature at equilibrium

$$\overline{T^*} = \frac{1}{B}(Q(1 - \overline{\alpha}(\eta, \beta)) - A),$$

where $\overline{\alpha}(\eta, \beta) = \int_0^1 s(y, \beta)\alpha(y, \eta)\, dy$ is the weighted average albedo, a 7th degree polynomial in η (coefficients in β).

This in turn gives a formula for the equilibrium temperature profile

$$T^*(y, \eta, \beta) = \frac{Q}{B + C}\left(s(y, \beta)(1 - \alpha(y, \eta)) + \frac{C}{B}(1 - \overline{\alpha}(\eta, \beta))\right) - \frac{A}{B}.$$

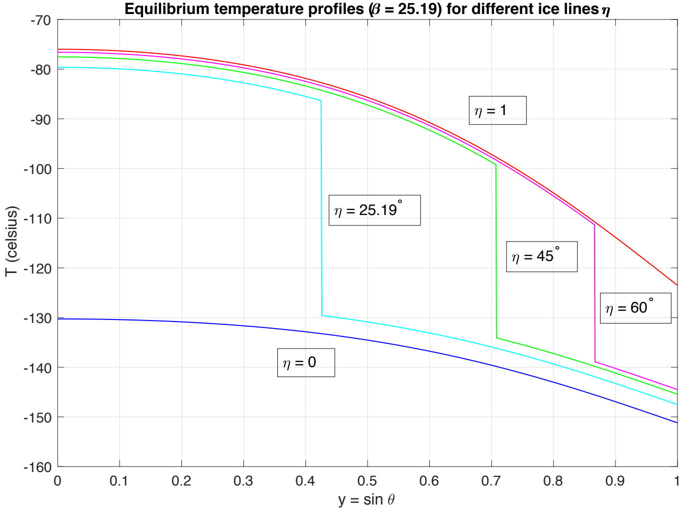

Figure: Graphs of equilibrium temperature profiles with two-step albedo function α_1 for obliquity $\beta = 25.19^\circ$ and various ice lines ($A = 230$, $C = 0.25$). $\eta = 1$ corresponds to an ice-free planet while $\eta = 0$ is ice-covered.

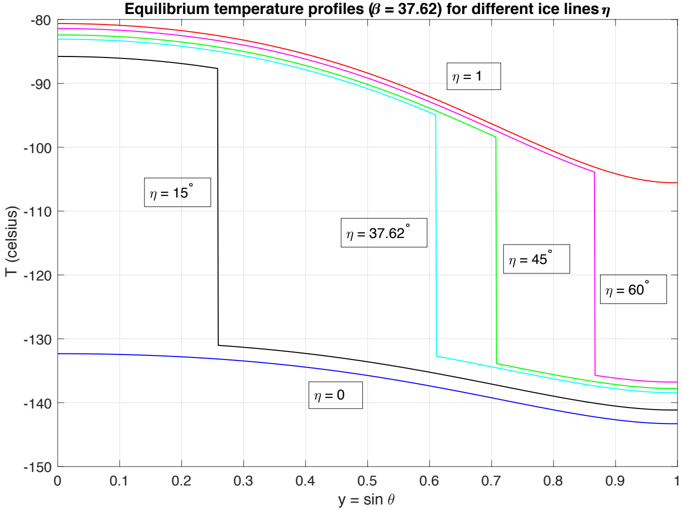

Figure: Graphs of equilibrium temperature profiles with two-step albedo function α_1 for obliquity $\beta = 37.62^\circ$ and various ice lines ($A = 230$, $C = 0.25$). $\eta = 1$ corresponds to an ice-free planet while $\eta = 0$ is ice-covered.

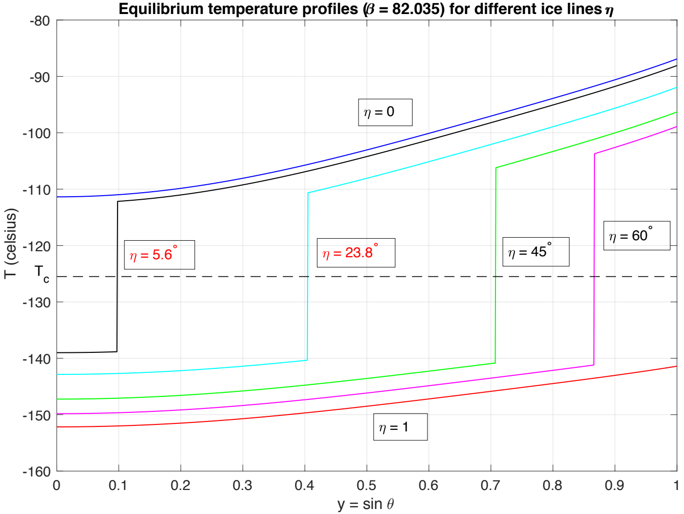

Figure: Graphs of equilibrium temperature profiles with two-step albedo function α_2 for obliquity $\beta = 82.035$ and various ice lines ($A = 245$, $C = 0.6$). Here, $\eta = 1$ corresponds to an ice-covered planet while $\eta = 0$ is ice-free.

Widiasih's Extension of Budyko Model (2013)

Recall that $T_c = -125.5°$C is the critical temperature at which CO_2 ice can form.

Treat the ice line η as a variable and append the ODE

$$\frac{d\eta}{dt} = \pm\epsilon(h(\eta,\beta) - T_c)$$

to the Budyko model, where ϵ is a small parameter and

$$\begin{aligned} h(\eta,\beta) &= T^*(\eta,\eta,\beta) = \frac{1}{2}\left(\lim_{y\to\eta^-} T^*(y,\eta,\beta) + \lim_{y\to\eta^+} T^*(y,\eta,\beta)\right) \\ &= \frac{Q}{B+C}\left[s(\eta,\beta)\left(1 - \frac{\alpha_r + \alpha_s}{2}\right) + \frac{C}{B}(1 - \overline{\alpha}(\eta,\beta))\right] - \frac{A}{B} \end{aligned}$$

is the equilibrium temperature at the ice line (7th-degree poly. in η). Choose $+$ for smaller obliquities and $-$ for larger ($\beta > \beta_c = 53.937°$).

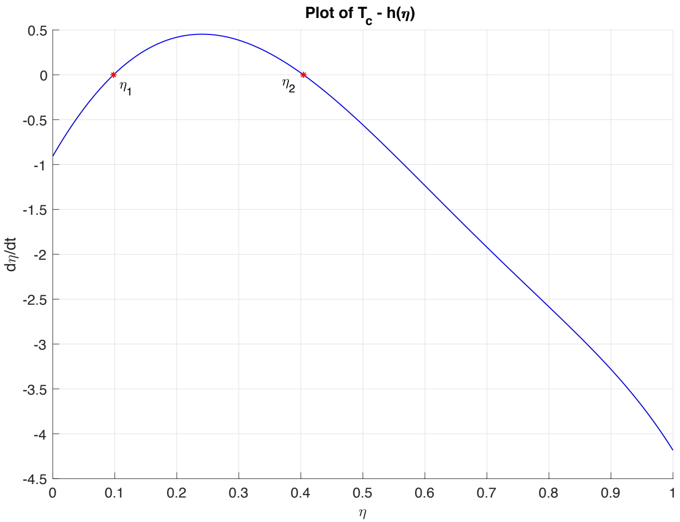

Figure: Plot of $T_c - h(\eta, \beta)$ for the Widiasih ice line equation $d\eta/dt = -\epsilon(h(\eta) - T_c)$ with $\beta = 82.035°$. Two equilibria ice lines exist at $\eta_1 \approx 0.0979$ (unstable) and $\eta_2 \approx 0.4042$ (stable ice belt).

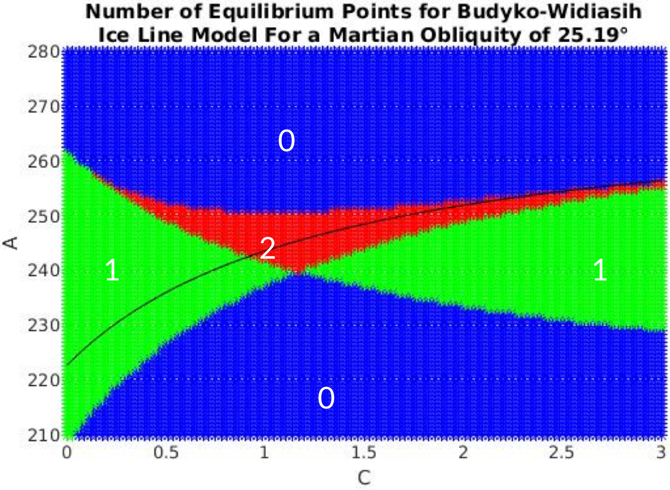

Figure: Bifurcation diagram indicating the number of ice line equilibria as A and C are varied for $\beta = 25.19°$. Red region yields stable and unstable ice caps. Black line indicates parameter values with an equilibrium point at the current Martian ice line (stable in our model). Figure by Ryan Ferraro.

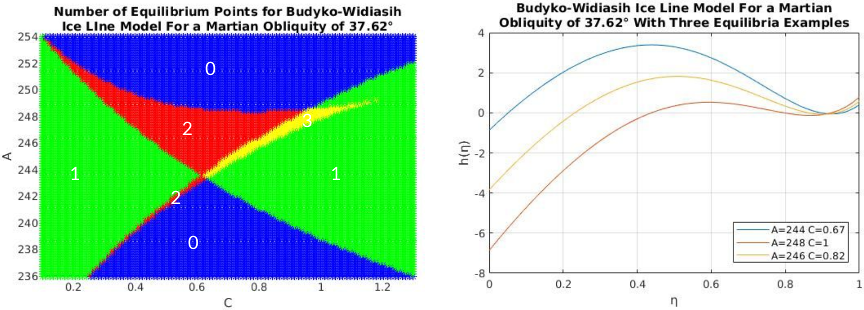

Figure: Bifurcation diagram (left) indicating the number of ice line equilibria as A and C are varied for $\beta = 37.62^\circ$. Yellow region yields 1 stable and 2 unstable equilibrium ice lines. Graphs of $h(\eta) - T_c$ (right) demonstrating a saddle node bifurcation.

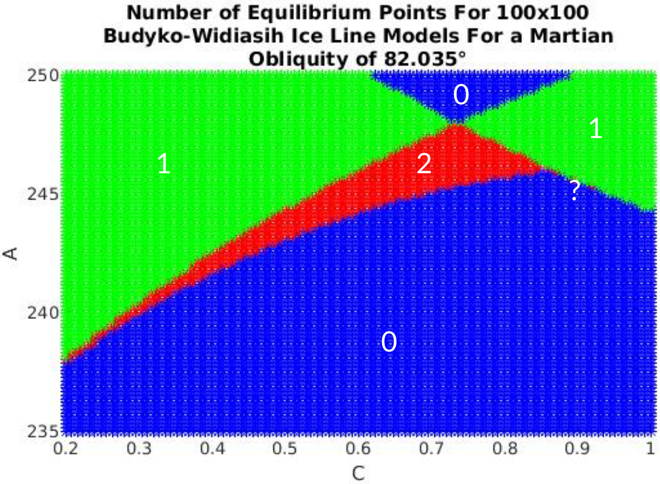

Figure: Bifurcation diagram indicating the number of ice line equilibria as A and C are varied for $\beta = 82.035°$, with adjusted albedo function α_2. Red region yields stable and unstable ice belts.

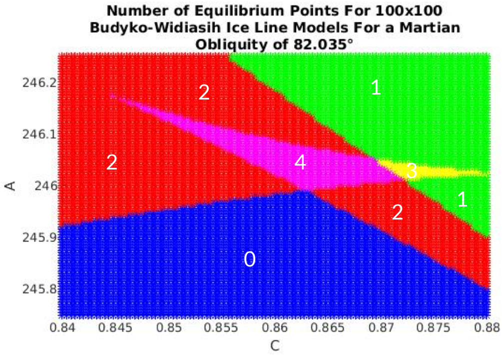

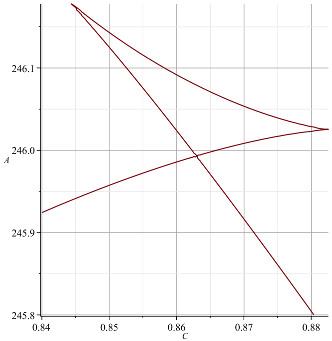

Figure: (Left) Zoom of previous diagram indicating parameter values with four equilibrium ice lines! A double saddle node bifurcation occurs at $A \approx 245.9931$ and $C \approx 0.8629$. (Right) Maple plot of the level curve $g(A, C) = 0$ where g is the discriminant of $h(\eta, \beta = 82.035) - T_c$ with respect to η. Any point on this level curve corresponds to parameter values with multiple roots (saddle node bifurcation). g is an 18th degree polynomial in A and C with 85 terms.

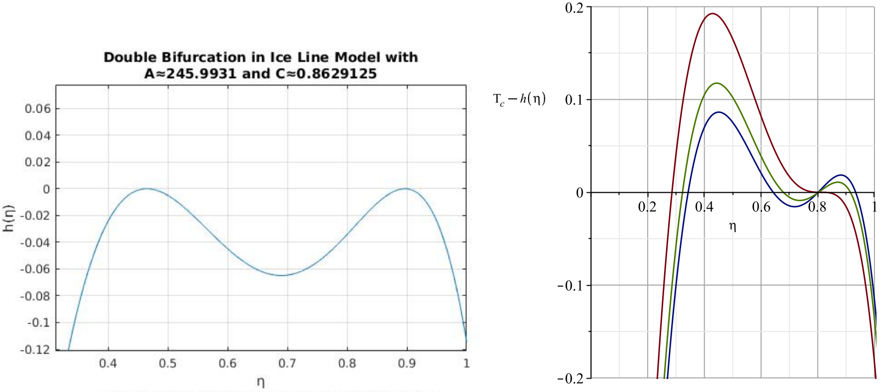

Figure: (Left) Graph of $T_c - h(\eta)$ at the double saddle node bifurcation. (Right) Graphs of $T_c - h(\eta)$ near $A \approx 246.1905$, $C \approx 0.84286$ illustrating a pitchfork bifurcation (cubic tangency).

Conclusion/Future Work

- The Budyko-Widiasih model applied to Mars in its current state yield stable and unstable ice caps for certain regions of parameter space.
- Incorporating the Nadeau-McGehee insolation approximation leads to more complicated dynamics and bifurcation scenarios, particularly for large obliquities where stable ice bands can form about the equator.
- Future work: Examine persistence of the bifurcations in terms of the obliquity β. What is the mathematical framework for the discontinuity separating small and large obliquities?
- Future work: Introduce asymmetry into the model by considering two dynamic ice lines η_S and η_N, where $\eta_S \leq \eta_N$.
- Thank you for your attention!

References

1. Armstrong, J. C., Conway, B. L., Quinn, T., A 1 Gyr climate model or Mars: new orbital statistics and the importance of seasonally resolved polar processes, *Icarus* **171** (2004), 255–271.
2. Laskar, J., Correia, A. C. M., Gastineau, M., Joutel, F., Levrard, B., Robutel, P., Long term evolution and chaotic diffusion of the insolation quantities of Mars, *Icarus* **170** (2004), 343–364.
3. Nadeau, A., McGehee, R., A simple formula for a planet's mean annual insolation by latitude, *Icarus* (2017), 46–50.
4. Postawko, S. E., Kuhn, W. R., Effect of the greenhouse gases (CO_2, H_2O, SO_2) on Martian paleoclimate, *J. Geophysical Research: Solid Earth* **91**, no. B4 (1986), D431–D438.
5. Rose, B. E. J., Cronin, T. W., Bitz, C. M., Ice caps and ice belts: The effects of obliquity on ice-albedo feedback, *The Astrophysical Journal* **846:28** (2017), 17pp.
6. Walsh, J., McGehee, R., Modeling Climate Dynamically, *The College Mathematics Journal* **44**, no. 5 (2013), 350–363.
7. Walsh, J., Widiasih, E., A Dynamics Approach To A Low-Order Climate Model, *Discrete and Continuous Dynamical Systems Series B* **19**, no. 1 (2014), 257–279.